JOURNAL OF GEOPHYSICAL RESEARCH, VOL. 92, NO. C9, PAGES 9531-9540, AUGUST 15, 1987

Infragravity Waves Over a Natural Barred Profile

ASBURY H. SALLENGER, JR.

U.S. Geological Survey, Reston, Virginia

ROBERT A. HOLMAN

College of Oceanography, Oregon State University, Corvallis

Measurements of cross-shore flow were made across the surf zone during a storm as a nearshore bar became better developed and migrated offshore. Measured infragravity band spectra were compared to synthetic spectra calculated numerically over the natural barred profile assuming a white run-up spectrum of leaky mode or high-mode edge waves. As in earlier studies, the spectra compared closely; however, for some frequencies the energy of the measured spectrum exceeded the energy of the synthetic spectrum, suggesting that the run-up spectrum was not white but had dominating frequencies. Utilizing cross-shore flow data and synthetic spectra from a number of cross-shore locations, an equivalent run-up spectrum was calculated for each day. On the first day of the storm, the equivalent run-up spectrum indicated a dominant wave that had a node in velocity reasonably close to the bar crest. Later during the storm, when the bar had migrated farther offshore, there was no evidence for a dominant motion having a velocity node at the bar crest. The structure of the equivalent run-up spectrum compared well with spectra of direct measurements of run-up obtained several hundred meters away. We have no clear evidence in support of the theory that infragravity waves might form or force the offshore migration of a bar. To confirm this finding, longer records obtained synoptically over a developing bar are required. The dominant wave observed early in the storm was consistent with Symond and Bowen's (1984) theoretical prediction of resonant amplification of discrete frequencies over a barred profile.

INTRODUCTION

The significance in the surf zone of infragravity waves, frequency band 0.05 to 0.005 Hz, is well recognized. Infragravity energy is not limited by wave breaking but rather becomes increasingly important close to the shoreline as offshore wave energy increases [e.g., *Suhayda*, 1974; *Guza and Thornton*, 1982, 1985; *Wright et al.*, 1982; *Holman and Sallenger*, 1985; *Sallenger and Holman*, 1985*b*]. In contrast, the energy of incident waves in the frequency band of about 1.0 to 0.05 Hz is limited by breaking and decreases with depth independent of offshore wave energy [e.g., *Thornton and Guza*, 1983; *Wright et al.*, 1982; *Vincent*, 1985; *Sallenger and Holman*, 1985*a*]. As a consequence, close to the shoreline, infragravity wave energy can dominate energy of incident waves. For an extreme example, run-up spectra measured on a high-energy beach by *Holman and Bowen* [1984] had 99.9% of their variance associated with frequencies lower than 0.05 Hz and 83% associated with frequencies lower than 0.02 Hz.

Several theories of nearshore bar formation involve waves in the infragravity band: either edge waves or leaky waves. Edge waves are waves progressive longshore and trapped to the nearshore by refraction, whereas leaky waves are reflected at the shoreline forming a standing wave pattern with the reflected wave "leaking" energy to the offshore. A leaky wave could set up a pattern of mass transport which potentially could form bars at nodes, or antinodes, of the standing wave motion [*Carter et al.*, 1973; *Lau and Travis*, 1973; *Bowen*, 1980]. Similarly, a progressive edge wave could form a linear, shore parallel bar, whereas an edge wave standing in the longshore could form a crescentic bar [*Bowen and Inman*, 1971; *Holman and Bowen*, 1982]. Once established, a bar may trap surface elevation antinodes of different wave frequencies; this may maintain the bar as conditions change [*Kirby et al.*, 1981].

Critical to the bar formation theories is the presence of a dominant infragravity wave at a discrete frequency, although in most field studies, the infragravity band has been found to be very broad [e.g., *Holman*, 1981; *Guza and Thornton*, 1982]. For broadband waves without a dominating frequency, nodes and antinodes associated with edge or leaky waves occur everywhere across the surf zone, and no bar would form. The presence of a bar may itself lead to the creation of a dominant infragravity wave. There could be seiching between shoreline and bar which could amplify frequencies with a node, or antinode, at the bar crest. In a theoretical study, *Symonds and Bowen* [1984] found for leaky waves and a linear, shore parallel bar that the resonant frequency should have a node in velocity at the bar crest. No theoretical evidence for resonance was found for frequencies with an antinode in velocity at the bar crest. *Huntley* [1980] presented some field evidence that a crescentic bar caused an edge wave of the same wavelength. *Wright et al.* [1986] presented field evidence suggesting the presence of a dominant wave having a node in velocity near the bar crest.

A first step toward determining whether infragravity waves form bars or whether bars amplify discrete infragravity frequencies is to examine infragravity motions over a barred profile. In this paper, we will show that there were dominant motions in the infragravity band over a barred profile during a storm, although the dominant motions were not always present. The main point of our paper is that when present, the dominant motion appeared to have a node in velocity close to the bar crest consistent with resonance. First we present theory on infragravity waves in the surf zone and discuss methods we used to determine dominant motions. After dis-

Paper number 7C0417.
0148-0227/87/007C-0417$05.00

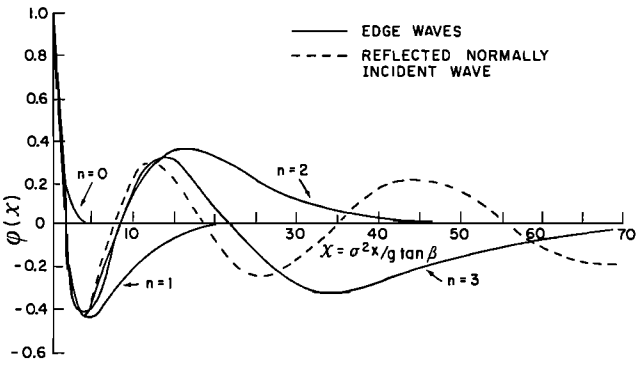

Fig. 1. Cross-shore behavior of edge waves (modes 0–3) and leaky waves plotted in terms of a nondimensional offshore distance, χ.

cussing the experimental setup, we present results describing the dominant waves in the surf zone and how the cross-shore structure of these waves related to morphology. In the discussion we speculate on the apparent lack of influence infragravity waves had in forcing offshore migration of the bar during the storm.

Theory

Using linear, shallow water equations of motion, *Ursell* [1952] found that on a plane beach an edge wave has a velocity potential given by

$$\Phi(x, y\ t) = (a_n g/\sigma)\ \phi_n(x) f(y, t) \tag{1}$$

where x and y are horizontal coordinates in the offshore and longshore directions, a is edge wave amplitude, g is acceleration of gravity, σ is radial frequency, n is modal number, and

$$f(y, t) = \cos(ky - \sigma t) \tag{2}$$

for progressive edge waves and

$$f(y, t) = \cos(ky) \cos(\sigma t) \tag{3}$$

for standing edge waves. The solution requires that the dispersion relation be given by

$$\sigma^2 = gk \sin(2n + 1)\beta \tag{4}$$

where β is beach slope. The offshore behavior of the edge wave is given by

$$\phi(x) = e^{-kx} L_n(2kx) \tag{5}$$

where L_n is the Laguerre polynomial of order n. The first four modes are plotted in Figure 1 against χ, the nondimensional offshore distance. Also plotted in Figure 1 is the offshore behavior of a leaky wave. For edge waves of mode above 1, the nearshore behavior of edge and leaky waves is about the same. Thus for example, a linear bar formed, say, at the first node of a leaky wave would form at essentially the same position for a high-mode progressive edge wave.

To detect dominant infragravity wave motions, we examine wave time series from instruments. It is apparent from Figure 1 and from (5) that if the instrument is at some offshore position x_i, an artificial spectral structure will be introduced. At certain frequencies, corresponding to nodes, no wave energy will be seen, while other frequencies, corresponding to antinodes, will exhibit a maximum in the spectrum. This apparent spectral structure is an artifact of the sampling and does not reflect true variations in energy.

The only location where no artificial structure is produced is at the shoreline where $\phi(x = 0) = 1.0$ for all frequencies. Thus we would like to examine run-up time series $R(t)$. Unfortunately, no run-up data were available at the longshore location of the main experiment, so that an "equivalent" run-up spectrum must be calculated based on the cross-shore flow data from offshore instruments.

Cross-shore velocity is given by

$$u(x, y, t) = \int_{-\infty}^{\infty} U(x, y, \sigma) e^{i\sigma t}\, d\sigma \tag{6}$$

where $U(x, y, \sigma)$ are the complex Fourier coefficients from which the spectrum is derived as

$$S_u(x, y, \sigma) = T\ U\ U^* \tag{7}$$

where T is length of record. Inserting the progressive linear long-wave form, we find

$$S_u(x, y, \sigma) = S_r(y, \sigma)\ [(g/\sigma)\ (d\phi\ (x, \sigma, n)/dx)]^2 \tag{8}$$

That is, the spectrum of the run-up, $S_r(y, \sigma)$, will be modified in a way dependent on the cross-shore structure of the wave, $\phi(x, \sigma, n)$ which is functionally $\phi(x)$. Synthetic velocity spectra, $S_u^s(x, y, \sigma)$, were calculated from (8), where the run-up spectrum was assumed white with an amplitude of unity, $S_r(y, \sigma) = 1$. For the complex natural profiles considered here, $\phi(x)$ was calculated numerically following *Holman and Bowen* [1979]. Synthetic spectra were compared to measured velocity spectra, $S_u^m(x, y, \sigma)$, to examine whether the measured spectral structures are consistent with the valleys and peaks associated with standing motions. In addition, we used the measured velocity spectrum to calculate an "equivalent" run-up spectrum,

$$S_r^e(\sigma) = S_u^m(\sigma)/[(g^2/\sigma^2)\ (d\phi\ (x, \sigma, n)/dx)^2] \tag{9}$$

It is readily evident from Figure 1 that the denominator of (9) will have zeros (the wave has zero crossings), so that any noise in the measured velocity spectrum at these frequencies will be amplified inordinately. To avoid this problem, the calculation of (9) was considered only for frequency bands surrounding velocity antinodes. Band cutoffs were taken at 80% of peak power at antinodes of the synthetic spectra (90% gave essentially the same result). We filled the resulting gaps in the equivalent run-up spectrum with data taken at different offshore locations, so that a smooth spectrum was produced. Note that with data from many cross-shore locations available, there will be some bands in the spectrum for which more than one estimate is available. These have been averaged to yield the equivalent run-up spectrum.

Experiment

This work was part of the Duck82 experiment conducted during October 1982 at the Field Research Facility (FRF) of the U.S. Army Corps of Engineers Coastal Engineering Research Center at Duck, North Carolina. An overall description of the Duck82 experiment is given by *Mason et al.* [1985]. The FRF is located on a long, straight beach of a barrier island. During our experiment there was one well-developed bar.

Most of the data discussed here were obtained with the U.S. Geological Survey (USGS) sled system [*Sallenger et al.*, 1983]. The sled is towed offshore and is returned to the beach using a double-drum winch and triangular line arrangement. The sled

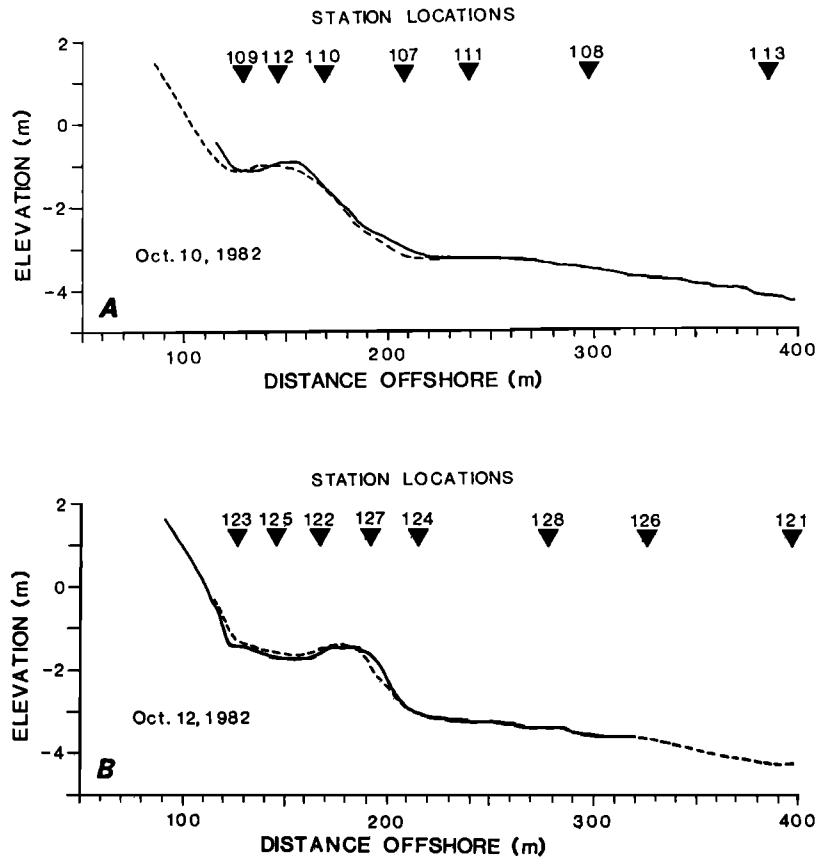

Fig. 2. (*a*) Station locations where flow measurements were obtained for October 10, 1982. The profiles were measured prior to the flow measurements (dashed line, 1130 EST) and near the end of flow measurements (solid line 1730 EST). Times of flow measurements are given in Figure 7. Distance offshore is relative to an arbitrary baseline. (*b*) Station locations for October 12, 1982. The profiles were measured prior to flow measurements (dashed line, 1345 EST) and following the flow measurements (solid line, 2110 EST). Times of flow measurements are given in Figure 8.

was set up 500 m north of the FRF pier to avoid the influence the pier has on flows and sediment transport [*Miller et al.*, 1983]. The nearshore profile was measured with an infrared rangefinder on the beach and optical prisms on top of the sled's mast. Mounted on the sled was a vertical array of Marsh-McBirney (model 512) electromagnetic flow meters (0.5, 1.0, and 1.75 m above the bottom) and a pressure sensor. These data were telemetered to shore. For the results discussed here, we used the records from the 1-m current meter, although the results would be essentially the same using either of the other meters. Data were recorded at 2 Hz for record lengths of 34.1 min. On each day of a storm, 7–8 records were taken across the nearshore profile, taking a total of approximately 5 hours. The plan was to bracket the daily measurement period around high tide, although as will be discussed later, this was not always possible. On each day, two measurements were obtained of the nearshore profile: one was prior to the flow measurements, and the other was near the end of the flow measurements.

Time series of run-up were measured at locations 300 m and

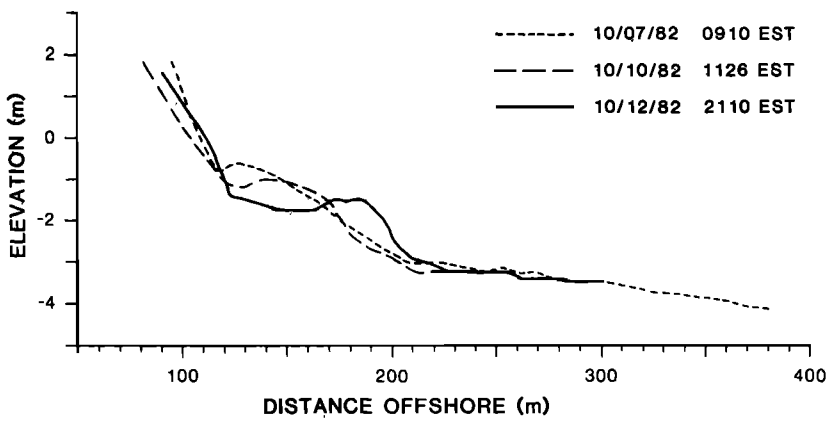

Fig. 3. Selected nearshore profile comparisons obtained through the storm of October 10–12, 1982. Offshore migration of the bar was not uniform through the storm. Most of the bar migration occurred between October 11 and 12, whereas little change occurred between October 10 and 11 [*Sallenger et al.*, 1985].

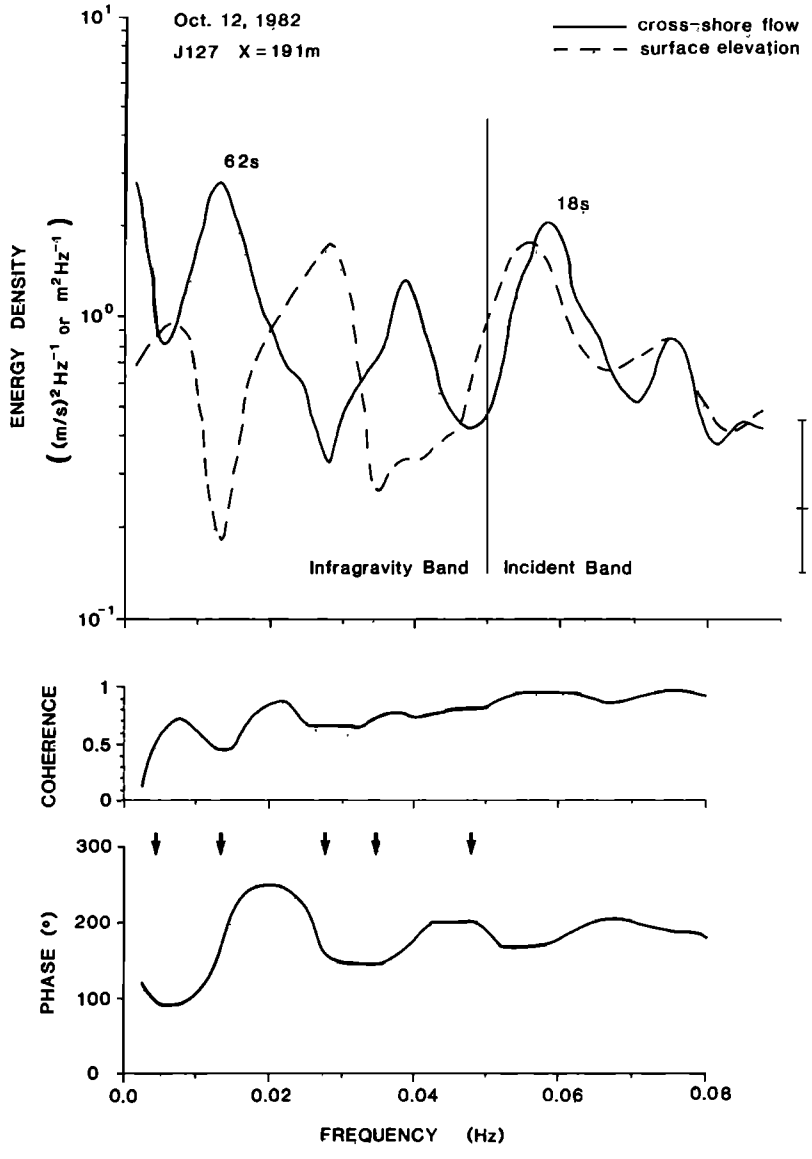

Fig. 4. Spectra of cross-shore flow and surface elevation, relative phase, and coherence, obtained at station J127. The arrows on the phase plot indicate frequencies of valleys (or nodes) of both flow and surface elevation.

more away from the sled line. The run-up records were 36 min long and were obtained using time-lapse photography as described by *Holman and Guza* [1984]. Owing to the long distance between measurements of run-up and measurements of morphology at the sled line, our interpretations of dominant motions were based on flow measurements at the sled, as well as the distant measured run-up.

RESULTS

The cross-shore flow data reported here were obtained during a 3-day storm (October 10–12, 1982) when significant breaker heights reached greater than 4 m and surf zone width was greater than 500 m [*Sallenger et al.*, 1985]. Flow measurements were from the inner 30–50% of the surf zone. Locations of each measurement station for the first and last day of the storm are shown in Figures 2*a* and 2*b*. The flow data were obtained over a nearshore bar that was in the process of migrating offshore (Figures 2 and 3). On a given day, flow records were measured sequentially (not synoptically), and were obtained at random offshore locations in the numerical order of station numbers to avoid introducing systematic bias caused by the offshore migrating bar. Prior to the storm, the bar was reasonably linear and shore parallel, whereas the waves were decreasing in height following the storm, the bar became increasingly crescentic. During the storm, we do not have complete data on three-dimensional morphology, although *Short* [1979] and others have suggested that under high-energy conditions, nearshore morphology tends to be linear. The storm-induced response of the nearshore morphology is discussed in more detail by *Sallenger et al.* [1985].

Infragravity band spectra of flow and surface elevation from the same location clearly indicate the presence of motions standing in the cross-shore (Figure 4). At frequencies where there are valleys in flow, suggesting velocity nodes, there are peaks in surface elevation, suggesting surface elevation antinodes, and vice versa. In the infragravity band, phase jumps occur consistently at frequencies associated with spectral valleys (nodes) of both surface elevation and flow. In the incident

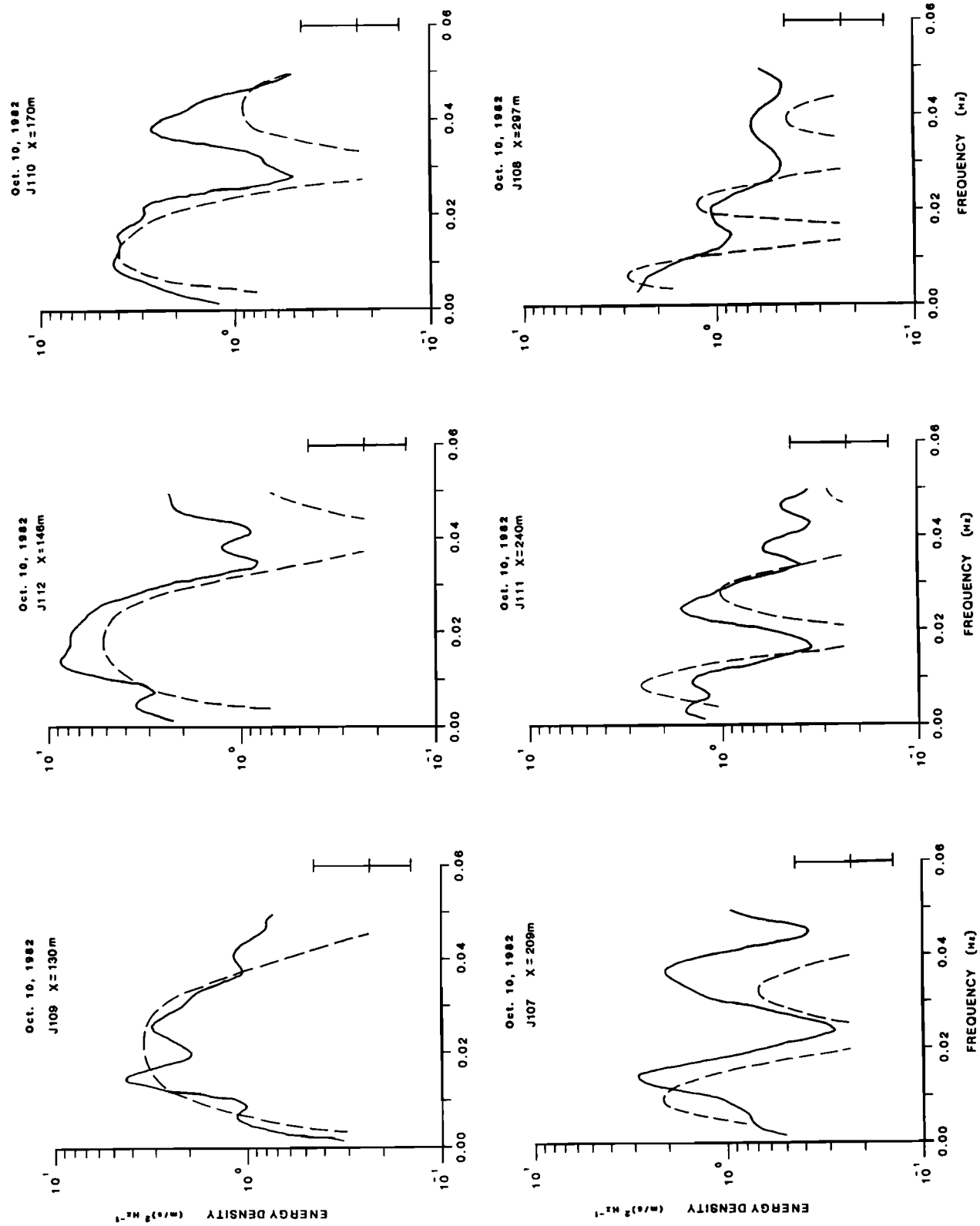

Fig. 5. Measured and synthetic cross-shore flow spectra for October 10, 1985. Spectra are plotted from the six stations closest to the beach. Confidence limits are 95%. The distance offshore, x, is given relative to an arbitrary baseline. The shoreline was approximately at $x = 110$ m.

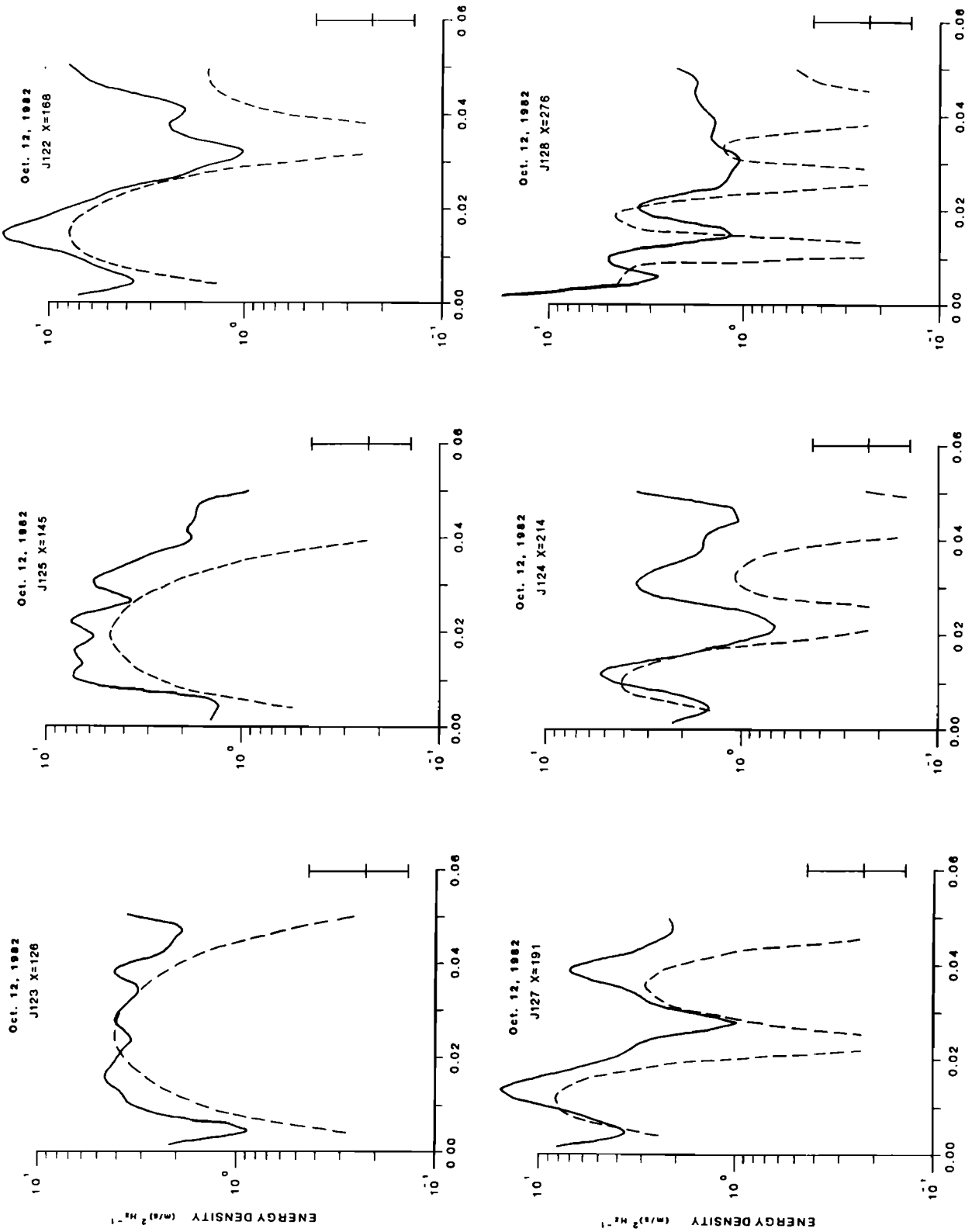

Fig. 6. Measured and synthetic cross-shore flow spectra for October 12, 1985. Spectra are plotted from the six locations closest to the beach. Confidence limits are 95%. The distance offshore, x, is given relative to an arbitrary baseline. The shoreline was approximately at $x = 110$ m.

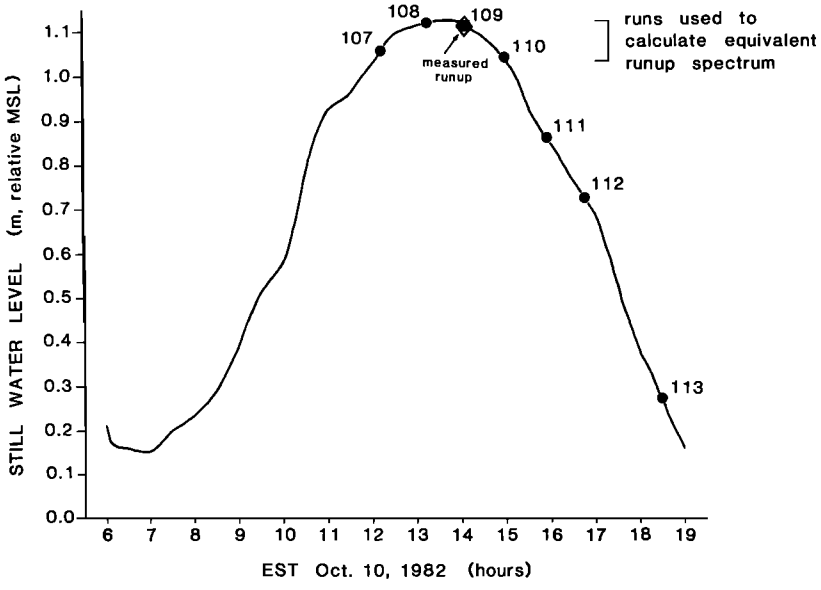

Fig. 7. Times of each data run for the first day of the storm (October 10) versus measured still water level. The open diamond indicates the time of the four synchronous run-up records.

band, relative phase approaches that expected for progressive waves. *Guza and Thornton* [1985] presented similar data pointing out the gradual change from distinct phase jumps at relatively low frequencies to an in-phase relationship between velocity and surface elevation at frequencies higher than that of the infragravity band.

Measured cross-shore flow spectra are plotted with synthetic spectra for the first day of the storm (October 10; Figure 5) and for the last day of the storm (October 12; Figure 6). In order to facilitate visual comparisons of infragravity band spectral structures, energy levels of synthetic spectra were adjusted by moving an entire spectrum vertically to fit the lower energy peaks of the measured spectrum. For a given set of spectra acquired on the same day, the spectra were all moved vertically the same amount. If there was a perfect fit between measured and synthetic spectra, the amount moved vertically would be $S_r(y, \sigma)$. As in earlier work, the synthetic spectra fit the measured spectra reasonably well, predicting frequencies of most major valleys and peaks [*Suhayda*, 1974; *Holman*, 1981; *Guza and Thornton*, 1985]. However, at some frequencies, energy levels of peaks rise higher than the synthetic spectra, indicating potential dominance at specific frequencies (e.g., Figures 5 (J110 and J107) and 6 (J127 and J124)).

The excellent agreement of the spectral structure (both phase and energy) to a standing wave model supports the use of equations (6)–(9) and allows the calculation of the equivalent run-up spectrum. To define the equivalent run-up spectrum from offshore stations, we require that the still water level during the offshore measurements remain stationary. On each day, the first four runs were completed during a period of small range in still water level (Figures 7 and 8). Using methods discussed in the "theory" section, estimates of $S_r^e(\sigma)$ were found using (9) for each of the stationary runs for each day (Figures 9*a* and 10*a*). For each day, the data were averaged to yield equivalent run-up spectra (solid lines in Figure 9*b* and 10*b*).

The equivalent run-up spectrum (solid line) for the first day of the storm indicates a dominant peak (0.036 Hz) that is significant at the 95% level (Figure 9*b*). As a check on our method for determining equivalent run-up spectra from offshore measurements, we compared the equivalent run-up spectrum at the sled line with four run-up spectra measured during the same period 300–375 m away from the sled line. No closer records were available. The run-up spectrum shown in Figure 9*b* (dashed line) is the average of the four spectra. Unlike the offshore data, run-up data were obtained synchronously and thus were not entirely independent realizations of the process. Consequently, confidence limits are likely narrower than the limit for individual spectra (noted by 1 in Figure 9*b*) but wider than the limit assuming individual spectra were independent (noted by 4, the number of spectra averaged). The structure of the measured run-up spectrum compares closely to the equivalent spectrum. Using the most stringent confidence limits, assuming degrees of freedom associated with individual spectra, the most energetic peak of the measured run-up spectrum

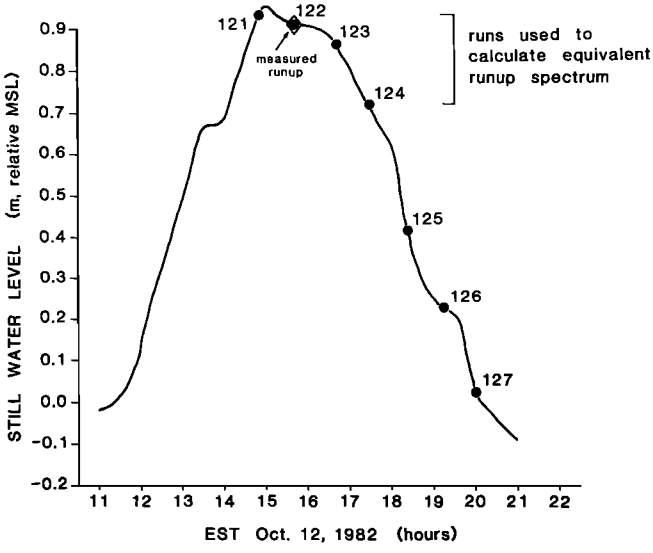

Fig. 8. Times of each data run for the last day of the storm (October 12) versus measured still water level. The open diamond indicates the time of the two synchronous run-up records.

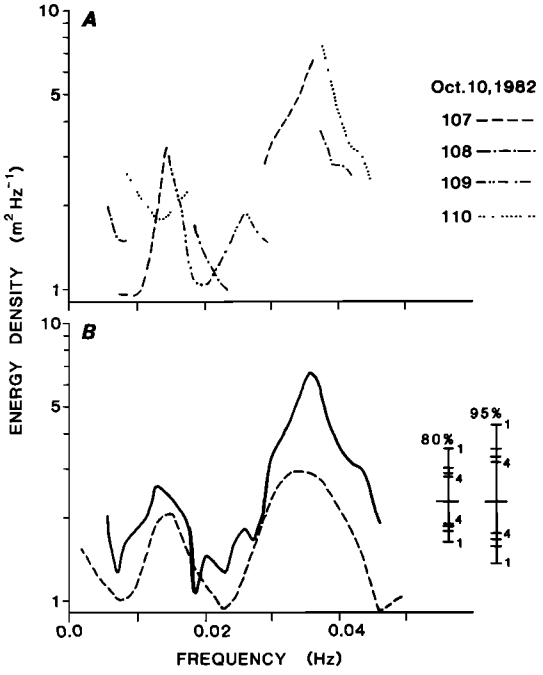

Fig. 9. Equivalent and measured run-up spectra for October 10. (*a*) Contribution of each offshore spectrum to the equivalent run-up spectrum. (*b*) The equivalent run-up spectrum is the solid line, and the measured run-up spectrum is the dashed line. The equivalent run-up spectrum is the average of the contributions of each offshore spectrum. Confidence limits associated with the equivalent run-up spectrum vary with frequency. The numbers adjacent to each limit refer to the number of offshore stations averaged. The number averaged can be determined from Figure 9*a*. The measured spectrum is the average of four spectra taken over a longshore distance of 75 m, each spectrum being 25 m apart. Unlike the offshore data, run-up data were obtained synchronously and thus were not entirely independent realizations of the process. Consequently, confidence limits are likely narrower than the limits for individual spectra (noted by 1, the number of spectra averaged) but wider than the limit assuming the individual spectra were independent (noted by 4).

is clearly significant at the 80% level and marginal at the 95% level. The frequency of the most energetic peak of the measured spectrum compares well with the frequency of the most energetic peak in the equivalent spectrum.

The structure of the wave associated with the dominant peak discussed above appears related to nearshore morphology (Figure 11). The curve shows predicted distances offshore (calculated numerically) to first nodes in cross-shore velocity. The datum point indicates the dominant frequency versus measured distance offshore to the bar crest. There appears to be a node in velocity reasonably close to the range in bar crest positions for the day. This is also shown in Figure 12, where we plot the cross-shore behavior of flow (and surface elevation) for the dominant frequency in relation to the measured nearshore profiles.

In contrast to the first day of the storm, on the last day there was no evidence for a significant peak at a frequency having a node in velocity at the bar crest (Figure 10*b*). Since the bar had moved offshore, a node at the bar crest would require a wave of lower frequency, 0.031 Hz. The equivalent runup spectrum in Figure 10*b* was not extended to 0.05 Hz because of data gaps (due to offshore instrument position) and because some frequencies were contaminated by incident band energy. The data gaps were filled using data from other tide levels (plot not shown). There still was no evidence for a peak near 0.031 Hz. In any case, there clearly is no evidence for a peak in the measured spectrum.

In addition to the clearly defined peak discussed above, there was some evidence for secondary peaks. On the first day, both equivalent and runup spectra indicate secondary peaks of lower frequency (0.013 Hz) and lower energy than the dominant peaks (Figure 9*b*). These secondary peaks are arguably significant at the 80% level. However, the structure of the motion is not closely related to bar morphology. On the last day, a peak close in frequency and energy to the secondary peak of the first day was present in the equivalent spectrum (and confident at 80%). Interestingly, a surface elevation node associated with this peak was reasonably close to the bar crest. However, confirmation of the peak on the last day was not present in the measured spectrum, which was not statistically different from white.

Discussion

We have no clear evidence supporting the hypothesis that infragravity waves can form or force the offshore migration of nearshore bars. On the first day of the storm there appeared to be a relationship between the bar position and the structure of a dominant infragravity wave. However, by the last day of the storm, there was no clear relationship consistent with the

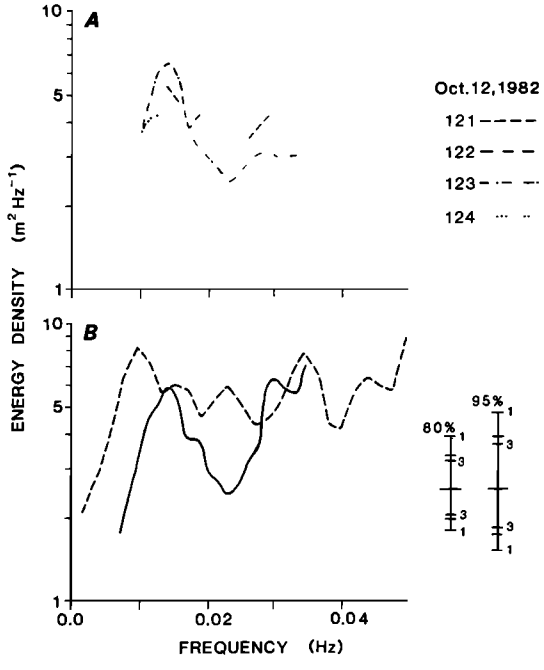

Fig. 10. Equivalent and measured run-up spectra for October 12. (*a*) Contribution of each offshore spectrum to the equivalent run-up spectrum. (*b*) The equivalent run-up spectrum is the solid line, and the measured run-up spectrum is the dashed line. The equivalent run-up spectrum is the average of the contributions of each offshore spectrum. Confidence limits associated with the equivalent run-up spectrum vary with frequency. The numbers adjacent to each limit refer to the number of offshore stations averaged. The number averaged varies with frequency and can be determined from Figure 10*a*. The measured spectrum is the average of two spectra (the only available ones) taken over a longshore distance of 75 m. Unlike the offshore data, run-up data were obtained synchronously and thus were not entirely independent realizations of the process. Consequently, confidence limits are likely narrower than the limits for individual spectra (noted by 1, the number of spectra averaged) but wider than the limits assuming the spectra were independent (noted by 2).

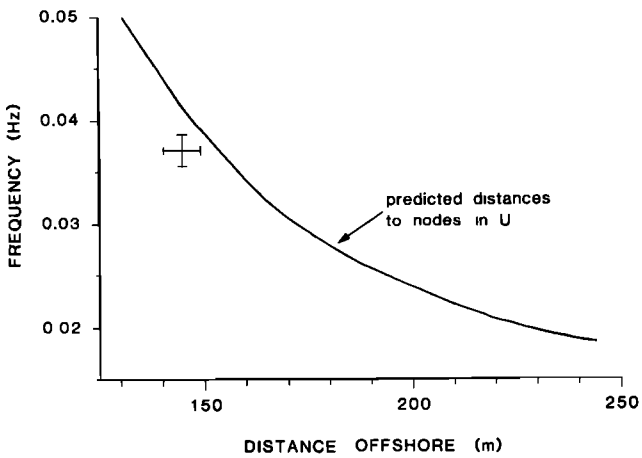

Fig. 11. The solid line indicates calculated positions of the first nodes of cross-shore flow for October 10. The datum point represents the range of distances offshore to bar crest for the two profiles measured on October 10 versus the dominant frequency found in the equivalent run-up spectrum. (See Figure 2 for details of profile measurements). The vertical bar indicates frequency resolution of the equivalent run-up spectrum, 0.0015 Hz.

first day. Note that the flow data on both days were obtained as the bar migrated offshore (Figure 2). If infragravity waves forced the observed offshore migration of the bar, we would expect dominant infragravity waves throughout the storm with consistent relationships between nodes (or antinodes) and the offshore migrating bar crest. As an alternative, perhaps a bar could be forced to migrate to a fixed node or antinode. There is some evidence for a secondary peak which persisted through the storm and, by the last day, had a surface elevation node close to the bar crest. However, such an interpretation is speculative, given the limited statistical confidence of the peaks and that on the last day the peak could not be found in the measured spectrum.

The dominance of a discrete frequency in the infragravity band on the first day of the storm is consistent with resonance since, as was predicted by *Symonds and Bowen* [1984], a node in velocity of the dominant wave appeared to be colocated with bar crest. However, by the last day of the storm, the resonance disappeared or at least was not strongly apparent within the statistical limits of the spectrum, even though a bar was still present. Perhaps, as the bar crest migrated into deeper water, the bar-trough morphology became less effective in trapping standing waves and in promoting resonance.

The records discussed here were 34 min long and were obtained sequentially across the nearshore profile not synoptically. Thus the statistical confidence of our spectra was limited, and the spectra may be affected by nonstationarity caused by time variations in the wave field and offshore migration of the bar. Longer records obtained synoptically over a developing bar would serve to confirm the results found here.

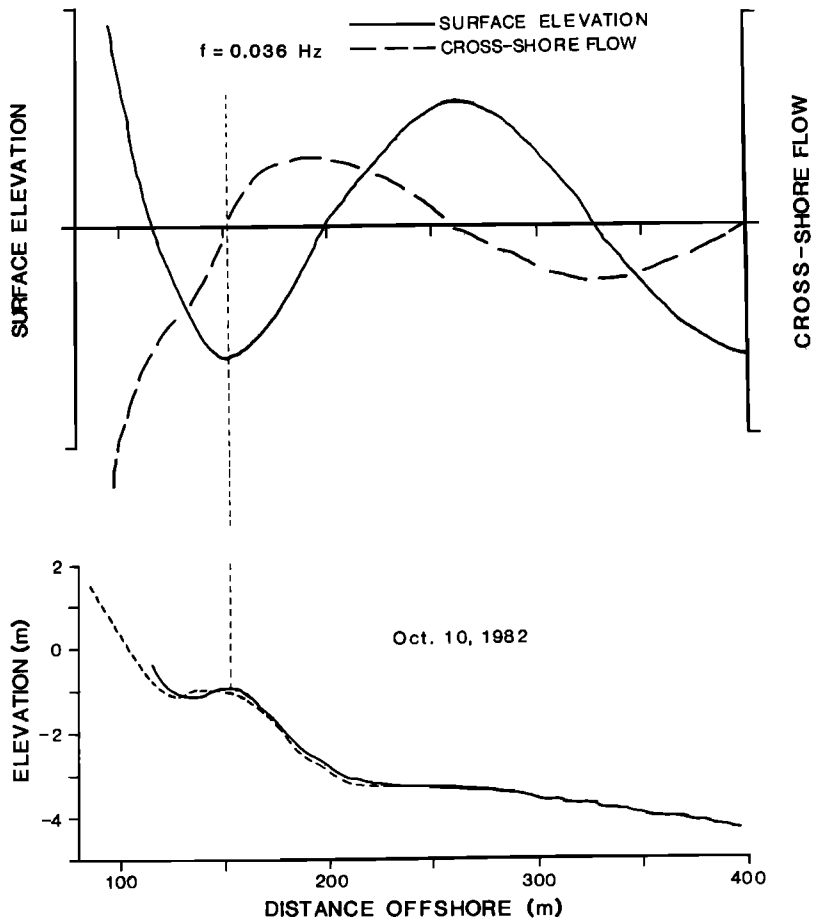

Fig. 12. (*a*) Cross-shore behavior of surface elevation and cross-shore flow (calculated using the numerical model) for the dominant peak found in the equivalent run-up spectrum for October 10. (*b*) Nearshore profiles from October 10, 1982. Elevation is in respect to mean sea level. The profiles were measured prior to the first flow measurement (dashed line, 1130 EST) and near the end of the flow measurements for the day (solid line, 1730). Times of flow measurements are given in Figure 7.

CONCLUSIONS

1. As was the case in earlier studies, infragravity-band waves, as seen in the cross-shore flow, had characteristics consistent with either high-mode edge waves or leaky mode waves.

2. Using offshore flow records over a barred profile, equivalent run-up spectra can be calculated. These equivalent spectra compare reasonably well with measured run-up spectra.

3. On the first day of a storm, equivalent run-up spectra indicated a dominant frequency that had a clear relationship with the bar. By the last day of the storm, there was no clear evidence of a dominant frequency that had a relationship with the bar consistent with the first day.

4. The dominant wave on the first day of the storm had a node in velocity close to the range in positions of the bar crest, consistent with the theoretical prediction of *Symonds and Bowen* [1984] that resonance on a barred profile could lead to amplification of discrete frequencies.

Acknowledgments. We thank Jeff List, Tom Reiss, Bruce Richmond, Bruce Jaffe, and Peter Howd for helping set up and operate the sled system, and Curt Mason and FRF crew for general support of the experiment. The acquisition of the data was funded jointly by the U.S. Geological Survey and the U.S. Army Engineer Waterways Experiment Station, Coastal Engineering Research Center, Vicksburg, MS. Data analyses and report preparation was supported primarily by USGS. We would also like to thank Office of Naval Research, Coastal Sciences program, contract N00014-84-0218, for additional support of the analyses. We thank Peter Howd and Bruce Jaffe for reviewing the manuscript.

REFERENCES

Bowen, A. J., Simple models of nearshore sedimentation, beach profiles and longshore bars, in *Coastline of Canada, Geol. Surv. Pap. Geol. Surv. Can., 80-10*, pp. 21–30, Geological Survey of Canada, Ottawa, 1980.

Bowen, A. J., and D. L. Inman, Edge waves and crescentic bars, *J. Geophys. Res., 76*, 8662–8671, 1971.

Carter, T. G., P. L. Liu, and C. C. Mei, Mass transport by waves and offshore sand bedforms, *J. Waterw. Harbors, Coastal Eng. Div. Am. Soc. Civ. Eng., 2*, 165–184, 1973.

Guza, R. T., and E. B. Thornton, Swash oscillations on a natural beach, *J. Geophys. Res., 87*(C1), 483–491, 1982.

Guza, R. T., and E. B. Thornton, Observations of surf beat, *J. Geophys. Res., 90*(C2), 3161–3172, 1985.

Holman, R. A., Infragravity energy in the surf zone, *J. Geophys. Res., 86*(C7), 6422–6450, 1981.

Holman, R. A., and A. J. Bowen, Edge waves on complex beach profiles, *J. Geophys. Res., 84*(C10), 6339–6346, 1979.

Holman, R. A., and A. J. Bowen, Bars, bumps, and holes: Models for the generation of complex beach topography, *J. Geophys. Res., 87*(C1), 457–468, 1982.

Holman, R. A., and A. J. Bowen, Longshore structure of infragravity wave motions, *J. Geophys. Res., 89*(C4), 6446–6452, 1984.

Holman, R. A., and R. T. Guza, Measuring run-up on a natural beach, *Coastal Eng., 8*, 129–140, 1984.

Holman, R. A., and A. H. Sallenger, Setup and swash on a natural beach, *J. Geophys. Res., 90*(C1), 945–953, 1985.

Huntley, D. A., Edge waves on a crescentic bar system, in *Coastline of Canada, Geol. Surv. Pap. Geol. Surv. Can., 80-10*, pp. 111–121, Geological Survey of Canada, Ottawa, 1980.

Kirby, J. T., R. A. Dalrymple, and L. F. Liu, Modification of edge waves by barred-beach topography, *Coastal Eng., 5*, 35–49, 1981.

Lau, J., and B. Travis, Slowly varying Stokes waves and submarine longshore bars, *J. Geophys. Res., 78*, 4489–4497, 1973.

Mason, C., A. H. Sallenger, R. A. Holman, and W. A. Birkemeier, A comprehensive experiment on storm-related coastal processes, in *Proceedings of the 19th Coastal Engineering Conference*, pp. 1913–1928, American Society of Civil Engineers, New York, 1985.

Miller, H. C., W. A. Birkemeier, and A. E. DeWall, Effects of CERC research pier on nearshore processes, in *Coastal Structures '83, Proceedings of the American Society of Civil Engineers*, pp. 769–784, American Society of Civil Engineers, New York, 1983.

Sallenger, A. H., and R. A. Holman, Wave energy saturation on a natural beach of variable slope, *J. Geophys. Res., 90*(C6), 11,939–11,944, 1985*a*.

Sallenger, A. H., and R. A. Holman, On predicting infragravity energy in the surf zone, in *Proceedings of the 19th Coastal Engineering Conference*, pp. 1940–1951, American Society of Civil Engineers, New York, 1985*b*.

Sallenger, A. H., P. C. Howard, C. H. Fletcher, and P. A. Howd, A system for measuring bottom profile, waves and currents in the high-energy nearshore environment, *Mar. Geol., 51*, 63–76, 1983.

Sallenger, A. H., R. A. Holman, and W. A. Birkemeier, Storm induced response of a nearshore-bar system, *Mar. Geol., 64*, 237–257, 1985.

Short, A. D., Three dimensional beach-stage model, *J. Geol., 87*, 553–571, 1979.

Suhayda, J. N., Standing waves on beaches, *J. Geophys. Res., 72*, 3065–3071, 1974.

Symonds, G., and A. J. Bowen, Interactions of nearshore bars with incoming wave groups, *J. Geophys. Res., 89*, 1953–1959, 1984.

Thornton, E. B., and R. T. Guza, Energy saturation and phase speeds measured on a natural beach, *J. Geophys. Res., 87*, 9499–9508, 1983.

Ursell, F., Edge waves on a sloping beach, *Proc. R. Soc. London, Ser. A, 214*, 79–97, 1952.

Vincent, C. L., Depth-controlled wave height, *J. Waterw. Port Coastal Ocean Div. Am. Soc. Civ. Eng., 111*(3), 459–475, 1985.

Wright, L. D., R. T. Guza, and A. D. Short, Dynamics of a high energy dissipative surf zone, *Mar. Geol., 45*, 41–62, 1982.

Wright, L. D., P. Nielsen, N. C. Shi, and J. H. List, Morphodynamics of a bar-trough surf zone, *Mar. Geol., 70*, 251–285, 1986.

R. A. Holman, College of Oceanography, Oregon State University, Corvallis, OR 97331.

A. H. Sallenger, Jr., U.S. Geological Survey, 914 National Center, 12201 Sunrise Valley Drive, Reston, VA 22092.

(Received June 20, 1986;
accepted November 10, 1986.)